

# Time-domain models for wave propagation in infinite beams

Peter Ruge, Carolin Birk

Lehrstuhl Dynamik der Tragwerke, Fakultät Bauingenieurwesen, Technische Universität Dresden, 01062 Dresden, Germany

*Abstract: In advanced structural dynamics coupled systems with bounded nonlinear members on the one side of the coupling interface and with unbounded linear elastic members on the other side are characterized by wave propagation and thus radiation damping. In this paper the dynamic stiffness for infinite beams in the frequency-domain is transformed into the time-domain using a rational approximation and following the mixed-variables formulation. Showing this process for Euler-Bernoulli's model and Timoshenko's shear model indicates significant differences with respect to analytical and numerical aspects.*

**Keywords:** radiation damping, dynamic stiffness approximation, Timoshenko beam, Euler-Bernoulli beam

## NOMENCLATURE

$\hat{F}$  = external force amplitude, [N]  
 $\hat{M}$  = external moment amplitude, [Nm]  
 $Q$  = shear force, [N]  
 $w$  = vertical displacement, [m]  
 $\mathbf{f}$  = force vector  
 $\mathbf{d}$  = deformation vector  
 $\mathbf{K}$  = dynamic stiffness matrix  
 $EI$  = flexural stiffness, [Nm<sup>2</sup>]  
 $A$  = cross-sectional area, [m<sup>2</sup>]  
 $G$  = shear modulus, [N/m<sup>2</sup>]  
 $q$  = distributed vertical load, [N/m]  
 $m$  = distributed moment, [Nm/m]  
 $i$  = imaginary unit  
 $a$  = real part of complex number  
 $b$  = imaginary part of complex number  
 $c$  = wave propagation speed, [m/s]  
 $r$  = radius, [m]  
 $x$  = coordinate, [m]  
 $t$  = time, [s]  
 $K_F$  = vertical stiffness, [N/m]  
 $K_M$  = rotational stiffness, [Nm]  
 $D$  = rotational damping coefficient, [Ns]  
 $M$  = degree of rational approximation  
 $l$  = number of data points involved in least-squares procedure  
 $P_j, p_j$  = numerator coefficients of rational function,  $j = 0 \dots M - 1$

$Q_j, q_j$  = denominator coefficients of rational function,  $j = 1 \dots M$   
 $E_F$  = vertical error norm  
 $E_M$  = rotational error norm  
 $v_j$  = internal variables,  $j = 1 \dots M$   
 $s_0, s_1$  = coefficients of linear representation  
 $r$  = numerator polynomial of strictly proper remainder  
 $\mathbf{A}, \mathbf{B}$  = matrices of resulting system of first-order differential equations  
 $\mathbf{z}$  = state variables  
 $\mathbf{r}$  = right-hand side vector  
 $n$  = integer number related to degree of fractional differentiation  
 $i_0$  = initial momentum, [Nms]  
 $h$  = time step size, [s]  
 $K$  = stiffness of rotational spring, [Nm]

### Greek Symbols

$\nu$  = Poisson's ratio  
 $\kappa$  = shear coefficient  
 $\phi$  = angle of rotation  
 $\gamma$  = shear angle  
 $\rho$  = mass density, [kg/m<sup>3</sup>]  
 $\mu$  = mass per length, [kg/m]

$\beta$  = distributed stiffness, [N/m<sup>2</sup>]  
 $\lambda$  = square of wave number  
 $\omega$  = excitation frequency, [1/s]  
 $\tilde{\omega}$  = cutoff frequency, [1/s]  
 $\Delta\omega$  = frequency increment, [1/s]  
 $\eta$  = dimensionless frequency (Timoshenko beam)  
 $\tilde{\eta}$  = dimensionless cutoff frequency (Timoshenko beam)  
 $\theta$  = dimensionless frequency (Euler-Bernoulli beam)  
 $\alpha$  = degree of fractional derivative  
 $\tau$  = time, [s]

### Subscripts

$T$  = translational properties  
 $R$  = rotational properties  
 $T\beta$  = translation + effect of distributed stiffness  
 $F$  = with respect to force  
 $M$  = with respect to moment

### Superscripts

$\infty$  = asymptotic,  $\omega \rightarrow$  infinity  
 $(i)$  = step of successive splitting procedure,  $i = 1 \dots M - 1$

## INTRODUCTION

Wave propagation and thus radiation damping plays a keyrole in structural dynamics with infinite members like soil, fluid, air or a concrete track of railways. In this context, the correct description of radiation damping is still a challenge. Conventional finite element models cause reflections of outgoing waves at artificial boundaries which have to be prevented by special measures. Summaries of such absorbing or transmitting boundaries can be found in (Wolf, 1986), (Kausel, 1988) and (Givoli, 1999). A well established method for the analysis of dynamic problems including unbounded media is the boundary element method (Beskos, 1987; Beskos, 1997). Here, the radiation condition is fulfilled by the fundamental solution explicitly. However, the numerical evaluation of the corresponding dynamic stiffness in the frequency-domain is a rather troublesome process and the transformation into the time-domain involving convolution is computationally expensive. The idea of extending the finite element mesh towards infinity has driven the development of infinite element techniques (Bettess, 1992). Although this method is well established in acoustics (Harari, 2006), only few applications to elastodynamic problems can be found in the literature.

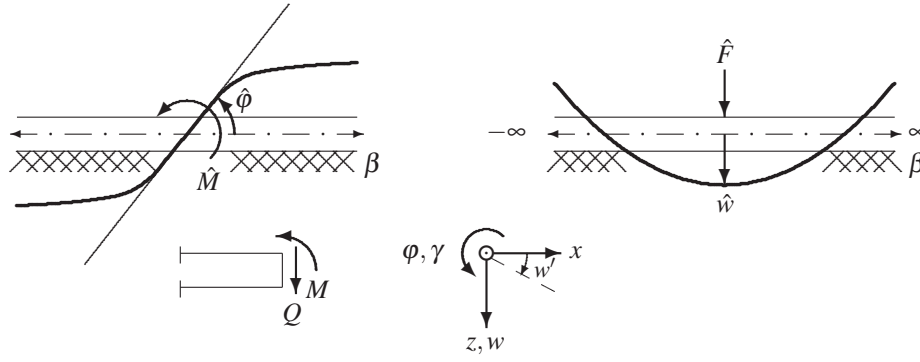


Figure 1 – Infinite Timoshenko beam. Definition of forces and deformations

A relatively recent method particularly suitable for the numerical solution of dynamic problems involving unbounded domains is the scaled boundary finite element method (SBFEM). This procedure has been developed within the last ten years by Wolf and Song (Song and Wolf, 1997; Wolf, 2003). The SBFEM is based on the use of scaled coordinates which allow the governing formulations to be discretized in the circumferential directions. The resulting ordinary differential equations for the dynamic stiffness or displacements with respect to the radial coordinate can then be solved in closed-form in the frequency-domain.

For infinite beams such ODEs in the space-domain appear a priori, their solution in the frequency-space-domain can be formulated analytically and the transformation into the time-domain can be organized without convolution using the 'mixed-variables technique' developed by Ruge and co-workers (Ruge, Trinks and Witte, 2001). Time-domain formulations should be able to describe the reaction of a structure even for transient excitations like impacts or start-ups and shut-downs of rotors. These are inputs with a frequency content which tends towards infinity. Consequently, the formulation in the frequency-domain should contain the asymptotic behaviour for  $\omega$  tending towards infinity. Thus, the dynamic analysis of infinite beam problems should use such mechanical models which are able to describe vibrations in the high-frequency range. For this purpose, Timoshenko's beam theory is more appropriate than Euler-Bernoulli's model as is shown in classical textbooks like (Fung, 1986). In addition, the asymptotic behaviour of Timoshenko's beam turns out to behave linear with respect to  $(i\omega)$ , whereas Euler-Bernoulli's model shows rational powers like  $(i\omega)^{\frac{1}{2}}$ ,  $(i\omega)^{\frac{3}{2}}$  which correspond to fractional derivatives in the time-domain. In addition to (Ruge and Birk, 2007), this contribution contains a comprehensive derivation of the dynamic stiffness matrix of beams bedded on a Winkler foundation. The asymptotic behaviour is addressed and the mixed-variables technique is summarized. The resulting state equations in the time-domain are discussed with respect to their numerical solution by local or non-local solvers and finally typical results are presented.

## INFINITE TIMOSHENKO BEAM

The dynamic behaviour of an infinite Timoshenko beam as shown in Fig. 1 is described and solved in the frequency-domain and used in order to formulate the dynamic stiffness relationship,

$$\begin{bmatrix} \hat{F} \\ \hat{M} \end{bmatrix} = \mathbf{K}(i\omega) \begin{bmatrix} \hat{w} \\ \hat{\phi} \end{bmatrix}, \quad \hat{\mathbf{f}} = \mathbf{K}\hat{\mathbf{d}}, \quad \mathbf{f}(t) = \hat{\mathbf{f}} \cdot e^{i\omega t}, \quad \mathbf{d}(t) = \hat{\mathbf{d}} \cdot e^{i\omega t}, \quad (1)$$

between the deformations  $\hat{\mathbf{d}}$  and the generalized forces  $\hat{\mathbf{f}}$  in the point where  $\mathbf{f}(t)$  acts onto the beam. If shear deformations are included, the slope of the deflection curve  $w(x)$  depends not only on the rotation  $\phi$  of the beam cross-section but also on the shear angle  $\gamma$ :

$$\frac{\partial}{\partial x} w(x,t) = -\phi(x,t) - \gamma(x,t). \quad (2)$$

Bending moment  $M(x,t)$  and shear force  $Q(x,t)$  are related to the corresponding deformations,

$$\begin{aligned} M(x,t) &= EI \frac{\partial}{\partial x} \phi(x,t), \\ Q(x,t) &= -\kappa GA \gamma = \kappa GA \left[ \phi(x,t) + \frac{\partial}{\partial x} w(x,t) \right], \end{aligned} \quad (3)$$

where  $EI$  is the flexural stiffness,  $A$  the cross-sectional area,  $G$  the shear modulus from  $E = 2G(1 + \nu)$  with Poisson's ratio  $\nu$ , and  $\kappa$  is the shear coefficient.  $\kappa$  depends on the shape of the cross-section, Poisson's ratio and the considered frequency range. For circles, rectangles and thin-walled cross-sections, Cowper (Cowper, 1966) gave several relations. For high-frequency modes, values published by Mindlin (Mindlin and Deresiewicz, 1953) should be considered. The

elasticity equations (3) are coupled with the dynamic equilibrium concerning the forces and the moments,

$$\frac{\partial}{\partial x} Q(x,t) + q(x,t) - \beta w(x,t) = \rho A \frac{\partial^2}{\partial t^2} w(x,t), \quad (4)$$

$$\frac{\partial}{\partial x} M(x,t) - Q(x,t) + m(x,t) = \rho I \frac{\partial^2}{\partial t^2} \varphi(x,t), \quad (5)$$

where  $\rho$  [kg/m<sup>3</sup>] is the mass density per volume,  $I$  the moment of inertia about the y-axis through the centre of the cross-section,  $q(x,t)$  [N/m] is the prescribed distributed load on the beam,  $m(x,t)$  [Nm/m] the prescribed distributed moment along the beam and  $\beta$  [N/m<sup>2</sup>] the distributed stiffness.

The constitutive relations (3) together with the equations of motion (4), (5) define the governing differential equations for the displacements  $w(x,t)$  and the rotation  $\varphi(x,t)$  :

$$\begin{aligned} -\kappa GA(\varphi_{,x} + w_{,xx}) + \beta w + \rho A w_{,tt} &= q, \\ \kappa GA(\varphi + w_{,x}) - EI\varphi_{,xx} + \rho I\varphi_{,tt} &= m. \end{aligned} \quad (6)$$

A wave-type representation

$$\begin{bmatrix} w(x,t) \\ \varphi(x,t) \end{bmatrix} = \begin{bmatrix} \hat{w} \\ \hat{\varphi} \end{bmatrix} e^{-x\sqrt{\lambda}+st}, \quad s = i\omega, \quad (7)$$

solves the homogeneous part of Eqs. (6) yielding a quadratic equation for the roots  $\lambda$  :

$$\lambda^2 - \lambda \frac{S_T M_R + S_R M_T \beta}{S_T S_R} + \frac{M_T \beta (M_R + S_T)}{S_T S_R} = 0. \quad (8)$$

The new parameters are related to rotational ( $R$ ) and translational ( $T$ ) properties.

$$\begin{aligned} S_T &= \kappa GA, & M_T \beta &= \rho A s^2 + \beta, & c_T^2 &= \frac{\kappa G}{\rho}, & s &= i\omega, \\ S_R &= EI, & M_R &= \rho I s^2, & c_R^2 &= \frac{E}{\rho}. \end{aligned} \quad (9)$$

Introducing a dimensionless frequency  $\eta$ ,

$$\eta^2 = \frac{\omega^2}{\left(\frac{\beta}{\rho A}\right)} = \frac{S_T}{\beta} \frac{\omega^2}{c_T^2} \quad \rightarrow \quad s^2 = (i\omega)^2 = -\eta^2 c_T^2 \frac{\beta}{S_T}, \quad (10)$$

simplifies the formulation of the roots  $\lambda_1, \lambda_2$  of the characteristic equation (8):

$$\lambda_{1,2} = \frac{1}{2} \frac{\beta}{S_T} \left[ (1 - \eta^2) + \frac{c_T^2}{c_R^2} (-\eta^2 \pm \sqrt{R}) \right], \quad (11)$$

$$R = 4 \frac{A}{I} \frac{S_T}{\beta} \frac{c_R^2}{c_T^2} (\eta^2 - 1) + \left[ \frac{c_R^2}{c_T^2} (1 - \eta^2) + \eta^2 \right]^2 \quad (12)$$

The special value  $\eta^2 = 1$  (first cut-off frequency) is related to one zero eigenvalue:

$$\lambda_{1,2} = \frac{1}{2} \frac{\beta}{S_T} \frac{c_T^2}{c_R^2} (-1 \pm 1), \quad \lambda_1 = -\frac{\beta}{S_T} \frac{c_T^2}{c_R^2} = -\frac{\beta}{EA}, \quad \lambda_2 = 0 \quad (13)$$

A second situation with  $\lambda_2 = 0$  for taking the plus sign in equation (11) follows from

$$(1 - \tilde{\eta}^2) + \frac{c_T^2}{c_R^2} (-\tilde{\eta}^2 + \sqrt{R}) \stackrel{!}{=} 0, \quad (14)$$

which leads to

$$4 \frac{A}{I} \frac{S_T}{\beta} (\tilde{\eta}^2 - 1) = 4 \tilde{\eta}^2 (\tilde{\eta}^2 - 1), \quad (15)$$

and thus

$$\tilde{\eta}_1 = 1, \quad \tilde{\eta}_2^2 = \frac{A}{I} \frac{S_T}{\beta} \quad (16)$$

or

$$\tilde{\omega}_1^2 = \frac{\beta}{\rho A}, \quad \tilde{\omega}_2^2 = \frac{S_T}{\rho I} = \frac{\kappa GA}{\rho I} = c_T^2 \frac{A}{I}. \quad (17)$$

The second cut-off frequency,  $\tilde{\omega}_2$ , is the same as for an infinite Timoshenko beam without an elastic restraint  $\beta$ . As the solution (7) in the space-domain is related to  $\sqrt{\lambda}$ , a change of the sign of a real value  $\lambda_2 \in \mathbb{R}$  influences the character of the solution significantly. Altogether, the properties of  $\lambda_1, \lambda_2$  with respect to the cut-off frequencies  $\tilde{\omega}_1, \tilde{\omega}_2$  are as follows:

$$\tilde{\omega}_1 = \sqrt{\frac{\beta}{\rho A}}, \quad \tilde{\omega}_2 = \sqrt{\frac{\kappa GA}{\rho I}}; \quad \left\{ \begin{array}{ll} \omega < \tilde{\omega}_1 & : \lambda_{1,2} = a \pm ib; \quad a, b \in \mathbb{R}. \\ \omega = \tilde{\omega}_1 & : \lambda_1 = -\frac{\beta}{EA}, \quad \lambda_2 = 0. \\ \tilde{\omega}_1 < \omega < \tilde{\omega}_2 & : \lambda_1, \lambda_2 \in \mathbb{R}; \quad \lambda_1 < 0, \quad \lambda_2 > 0. \\ \omega = \tilde{\omega}_2 & : \lambda_1 \in \mathbb{R}, \quad \lambda_1 < 0, \quad \lambda_2 = 0. \\ \omega > \tilde{\omega}_2 & : \lambda_1, \lambda_2 \in \mathbb{R}; \quad \lambda_1 < 0, \quad \lambda_2 < 0. \end{array} \right. \quad (18)$$

With the help of  $\lambda_1, \lambda_2$  the normalized deformation  $w_F(r)$  for a unit force  $\hat{F} = 1[N]$  at  $r = 0, r = \sqrt{x^2}$ , and the normalized rotation  $\varphi_M(r)$  for a unit moment  $\hat{M} = 1[Nm]$  at  $r = 0$  can be described using Hörmander's theorem (Hörmander, 1963), elaborated by Antes (Antes, Schanz and Alvermann, 2004):

$$w_F = \frac{1}{2S_T(\lambda_1 - \lambda_2)} \left[ \frac{e^{-\sqrt{\lambda_1}r}}{\sqrt{\lambda_1}} \left( \lambda_1 - \frac{S_T + M_R}{S_R} \right) - \frac{e^{-\sqrt{\lambda_2}r}}{\sqrt{\lambda_2}} \left( \lambda_2 - \frac{S_T + M_R}{S_R} \right) \right], \quad (19)$$

$$\varphi_M = \frac{1}{2S_R(\lambda_1 - \lambda_2)} \left[ \frac{e^{-\sqrt{\lambda_1}r}}{\sqrt{\lambda_1}} \left( \lambda_1 - \frac{M_T\beta}{S_T} \right) - \frac{e^{-\sqrt{\lambda_2}r}}{\sqrt{\lambda_2}} \left( \lambda_2 - \frac{M_T\beta}{S_T} \right) \right]. \quad (20)$$

Due to  $K_F = \frac{\hat{F}}{w}$  and  $K_M = \frac{\hat{M}}{\varphi}$  at the point  $r = 0$  where  $\hat{F}$  and  $\hat{M}$  act onto the beam, the stiffnesses  $K_F, K_M$  follow directly from the solutions (19) and (20), respectively .

$$K_F = \frac{1}{w_F(r=0)} = \frac{2S_T(\lambda_1 - \lambda_2)\sqrt{\lambda_1\lambda_2}}{\sqrt{\lambda_2}\left(\lambda_1 - \frac{S_T + M_R}{S_R}\right) - \sqrt{\lambda_1}\left(\lambda_2 - \frac{S_T + M_R}{S_R}\right)}, \quad (21)$$

$$K_M = \frac{1}{\varphi(r=0)} = \frac{2S_R(\lambda_1 - \lambda_2)\sqrt{\lambda_1\lambda_2}}{\sqrt{\lambda_2}\left(\lambda_1 - \frac{M_T\beta}{S_T}\right) - \sqrt{\lambda_1}\left(\lambda_2 - \frac{M_T\beta}{S_T}\right)}, \quad (22)$$

Below the first critical frequency  $\tilde{\omega}_1$  both stiffnesses  $K_F$  and  $K_M$  are purely real-valued and indicate properties of a corresponding frequency-dependent spring. Above the second critical frequency  $\tilde{\omega}_2$  the stiffnesses are purely imaginary and indicate radiation damping which can be described by a constant damping coefficient when  $\omega$  tends towards infinity.

$$\lim_{\omega \rightarrow \infty} K_F = K_F^\infty = \frac{2S_T}{c_T} \cdot i\omega = 2A\sqrt{\kappa G\rho} \cdot i\omega, \quad (23)$$

$$\lim_{\omega \rightarrow \infty} K_M = K_M^\infty = \frac{2S_R}{c_R} \cdot i\omega = 2I\sqrt{E\rho} \cdot i\omega. \quad (24)$$

For the rotational degree of freedom, the relationship to viscous damping with the corresponding moment,

$$M(t) = D\dot{\varphi}(t), \quad (25)$$

in the time-domain follows directly from the assumption of a time-harmonic behaviour of both quantities,  $\varphi(t)$  as well as  $M(t)$ :

$$M(t) = \hat{M} \cdot e^{i\omega t}; \quad \varphi(t) = \hat{\varphi} \cdot e^{i\omega t}. \quad (26)$$

Thus, Eq. (25) in the time-domain corresponds to

$$\hat{M} = i\omega \cdot D\hat{\varphi} \quad (27)$$

in the frequency domain. Comparing Eqs. (23) and (27) yields a constant damping coefficient  $D = 2I\sqrt{E\rho}$  in case of the rotational stiffness for  $\omega$  tending towards infinity.

## Frequency-to-time transformation

The dynamic stiffnesses given in Eqs. (21) and (22) completely describe the relationship between a point load or moment, respectively and the resulting deformations at  $x = 0$  in the frequency-domain. However, for the analysis of transient dynamic problems, a direct time-domain model is desirable. In the preceding section it has been shown that Eqs. (21) and (22) can be interpreted as simple dampers in the time-domain for infinitely large excitation frequencies.

However, in general the stiffness formulations for the Timoshenko beam in the frequency-domain are rather complicated functions of the frequency:

$$\hat{F} = K_F(i\omega)\hat{w} = K_F^\infty\hat{w} + (K_F - K_F^\infty)\hat{w}, \quad K_F^\infty = i\omega \frac{2S_T}{c_T}; \quad (28)$$

$$\hat{M} = K_M(i\omega)\hat{\phi} = K_M^\infty\hat{\phi} + (K_M - K_M^\infty)\hat{\phi}, \quad K_M^\infty = i\omega \frac{2S_R}{c_R}. \quad (29)$$

Only the asymptotic parts  $K^\infty$  are simple linear functions with respect to  $(i\omega)$ . The so-called low-frequency parts  $K - K^\infty$  must tend towards zero for  $\omega$  tending towards infinity.

The frequency-to-time transformation of the Eqs. (28-29) is done in steps according to recent publications (Ruge, Trinks and Witte, 2001; Trinks, 2004)

**Step 1** Rational approximation of low-frequency parts  $K - K^\infty$ :

$$K_F - K_F^\infty = \frac{P_0 + (i\omega)P_1 + \dots + (i\omega)^{M-1}P_{M-1}}{1 + (i\omega)Q_1 + \dots + (i\omega)^M Q_M} = \frac{P(i\omega)}{Q(i\omega)}; \quad (30)$$

$$K_M - K_M^\infty = \frac{p_0 + (i\omega)p_1 + \dots + (i\omega)^{M-1}p_{M-1}}{1 + (i\omega)q_1 + \dots + (i\omega)^M q_M} = \frac{p(i\omega)}{q(i\omega)}. \quad (31)$$

The coefficients  $P_j, Q_j$  and  $p_j, q_j$  are found by minimizing the error-norms  $E_F, E_M$ :

$$\begin{aligned} E_F &= \|(K_F - K_F^\infty) - P(i\omega)/Q(i\omega)\|, \\ E_M &= \|(K_M - K_M^\infty) - p(i\omega)/q(i\omega)\|, \end{aligned} \quad (32)$$

using an amount of  $l + 1$  distinct values  $\omega_j = j\Delta\omega, j = 1, \dots, l$  with a frequency increment  $\Delta\omega$ .

**Step 2** Replacement of the fraction  $p/q$  by a new state variable  $v_1$  and changing from proper fraction  $p/q$  to improper fraction  $q/p$  (shown only for  $K_M$ ):

$$\begin{aligned} \hat{M} &= \left( i\omega \frac{2S_R}{c_R} \right) \hat{\phi} + \hat{v}_1, \\ \hat{v}_1 &= \frac{p(i\omega)}{q(i\omega)} \hat{\phi} \rightarrow \hat{\phi} = \frac{q(i\omega)}{p(i\omega)} \hat{v}_1. \\ \hat{v}_1 &: \text{first internal variable.} \end{aligned} \quad (33)$$

**Step 3** Splitting of  $q/p$  into a linear part with respect to  $i\omega$  and a strictly proper remainder:

$$\frac{q}{p} = s_0^{(0)} + i\omega s_1^{(0)} + \frac{r^{(0)}(i\omega)}{p(i\omega)}, \quad \frac{r^{(0)}(i\omega)}{p(i\omega)} : \text{proper fraction}, \quad (34)$$

$$\hat{\phi} = (s_0^{(0)} + i\omega s_1^{(0)})\hat{v}_1 + \hat{v}_2, \quad (35)$$

$$\hat{v}_2 = \frac{r^{(0)}}{p} \hat{v}_1 \rightarrow \hat{v}_1 = \frac{p}{r^{(0)}} \hat{v}_2, \quad \frac{p}{r^{(0)}} : \text{improper fraction}, \quad (36)$$

$$\hat{v}_2 : \text{second internal variable.} \quad (37)$$

**Further steps** Continuation of step 3 until the process ends up with a last linear part without an additional fraction.

Finally, a strictly linear representation with respect to  $i\omega$  with  $M$  additional internal variables is obtained:

$$(\mathbf{A} + i\omega\mathbf{B})\hat{\mathbf{z}} = \hat{\mathbf{r}}, \quad (38)$$

$$\mathbf{A} = \begin{bmatrix} 0 & 1 & 0 & \dots & 0 \\ 1 & -s_0^{(0)} & -1 & \dots & 0 \\ 0 & -1 & s_0^{(1)} & \dots & 0 \\ \vdots & \vdots & \vdots & \vdots & \vdots \\ 0 & 0 & \dots & \mp 1 & \pm s_0^{(M-1)} \end{bmatrix}, \quad \hat{\mathbf{z}} = \begin{bmatrix} \hat{\phi} \\ \hat{v}_1 \\ \hat{v}_2 \\ \vdots \\ \hat{v}_M \end{bmatrix}, \quad \hat{\mathbf{r}} = \begin{bmatrix} \hat{M} \\ 0 \\ 0 \\ \vdots \\ 0 \end{bmatrix}, \quad (39)$$

$$\mathbf{B} = \text{diag} \left\{ \frac{2S_R}{c_R}, -s_1^{(0)}, s_1^{(1)}, \dots, \pm s_1^{(M-1)} \right\}. \quad (40)$$

Assuming a harmonic behaviour of the state variables,

$$\mathbf{z}(t) = \hat{\mathbf{z}} \cdot e^{i\omega t}, \quad \mathbf{r}(t) = \hat{\mathbf{r}} \cdot e^{i\omega t}, \quad (41)$$

Eq. (38) corresponds to a first-order differential equation with respect to time:

$$\mathbf{A}\mathbf{z}(t) + \mathbf{B}\dot{\mathbf{z}}(t) = \mathbf{r}(t). \quad (42)$$

This ODE can be coupled to additional structural members (even with nonlinear behaviour) and solved in the time-domain with standard numerical time-stepping schemes.

## INFINITE EULER-BERNOULLI BEAM

The governing differential equation, here with an additional elastic Winkler foundation  $\beta$  [ $N/m^2$ ],

$$EIw_{,xxxx}(x,t) + \beta w(x,t) + \rho Aw_{,tt}(x,t) = 0, \quad (43)$$

is solved by exponential functions  $w(x,t) = \hat{w}e^{\lambda x}e^{i\omega t}$ . The dynamic stiffnesses  $K_F$  and  $K_M$  are derived in Ruge and Trinks (2003).

$$K_F = 8EIW^3, \quad (44)$$

$$K_M = 4EIW, \quad (45)$$

$$W = \frac{1}{2} \sqrt[4]{\frac{\beta}{EI}} \cdot \begin{cases} \sqrt{2} \sqrt[4]{1 - \theta^2} & \text{for } \theta^2 \leq 1 \\ (1+i) \sqrt[4]{\theta^2 - 1} & \text{for } \theta^2 > 1. \end{cases}, \quad \theta^2 = \omega^2 \frac{\rho A}{\beta}. \quad (46)$$

For  $\beta \rightarrow 0$  these values change into rational powers of the frequency (Ruge and Trinks, 2004):

$$K_F = 2\sqrt{2}EIC^{\frac{3}{4}}(i\omega)^{\frac{3}{2}}, \quad (47)$$

$$K_M = 2\sqrt{2}EIC^{\frac{1}{4}}(i\omega)^{\frac{1}{2}}, \quad C = \frac{\rho A}{EI}. \quad (48)$$

## Frequency-to-time transformation

The harmonic behaviour

$$\mathbf{d}(x,t) = \begin{bmatrix} w(x,t) \\ \varphi(x,t) \end{bmatrix} = \begin{bmatrix} w(x) \\ \varphi(x) \end{bmatrix} e^{i\omega t}, \quad \frac{\partial^\alpha}{\partial t^\alpha} \mathbf{d}(x,t) = (i\omega)^\alpha \mathbf{d}(x,t), \quad (49)$$

can be used to turn over from the frequency-domain descriptions (47), (48) for the infinite Euler-Bernoulli beam into the time domain.

$$\hat{F} = K_F \hat{w}, \quad \hat{M} = K_M \hat{\varphi},$$

$$F(t) = 2\sqrt{2}EIC^{\frac{3}{4}} \left[ -{}_{-\infty}D_t^{\frac{3}{2}} w(t) \right], \quad (50)$$

$$M(t) = 2\sqrt{2}EIC^{\frac{1}{4}} \left[ -{}_{-\infty}D_t^{\frac{1}{2}} \varphi(t) \right]. \quad (51)$$

Here, noninteger powers of  $(i\omega)$  have been interpreted as fractional derivatives of the unknowns  $\mathbf{z}(t)$ . This is based on the so-called Riemann–Liouville definition (52) of fractional differentiation which can be found in the textbook (Podlubny, 1999), for example.

$${}_aD_t^\alpha \mathbf{d} = \frac{1}{\Gamma(n-\alpha)} \frac{d^n}{dt^n} \int_a^t \frac{\mathbf{d}(\tau)}{(t-\tau)^{\alpha+1-n}} d\tau, \quad n-1 \leq \alpha \leq n. \quad (52)$$

In Eq. (52),  $n$  is an integer number. Application of definition (52) using the lower terminal  $a = -\infty$  to a harmonic function returns the latter together with a factor  $(i\omega)^\alpha$ .

$$-{}_{-\infty}D_t^\alpha \exp(i\omega t) = (i\omega)^\alpha \exp(i\omega t). \quad (53)$$

However, if the quantities  $\mathbf{d}$  between  $(t \rightarrow -\infty)$  and  $t = 0$ , where the system starts to exist, are identically zero, then the lower limit of the integral in Eq. (52) can be replaced by 0.

$$\mathbf{d}(t) \equiv \mathbf{0} \quad \text{for } -\infty < t \leq 0. \quad (54)$$

$$\rightarrow -{}_{-\infty}D_t^\alpha \mathbf{d} = \frac{1}{\Gamma(n-\alpha)} \frac{d^n}{dt^n} \int_0^t \frac{\mathbf{d}(\tau)}{(t-\tau)^{\alpha+1-n}} d\tau, \quad n-1 \leq \alpha \leq n.$$

Thus, the approach presented in this paper is limited to situations with zero initial conditions for the displacements and rotations. An initial momentum  $i_0$  [ $kg\,m^2\,s^{-1}$ ] can be modelled by applying a constant moment within a very short time interval  $h$ :  $i_0 = Mh$ .

### EXAMPLE

In order to illustrate the differences between the Timoshenko and Euler-Bernoulli beam models the specific system shown in Fig. 2 with the material data given in Eq. (55) has been analysed.

$$\begin{aligned} E &= 2.1 \cdot 10^{11} \text{ [N/m}^2\text{]}, \quad I = 2073 \text{ [cm}^4\text{]}, \quad \nu = 0.3, \\ A &= 6948 \text{ [mm}^2\text{]}, \quad \mu = \rho A = 54.5 \text{ [kg/m]}, \quad \kappa = \frac{5}{6}. \end{aligned} \quad (55)$$

Here, the distributed stiffness is replaced by a single rotational spring of stiffness  $K = 1.6 \cdot 10^7 \text{ Nm}$  at  $x = 0$ . The rotational

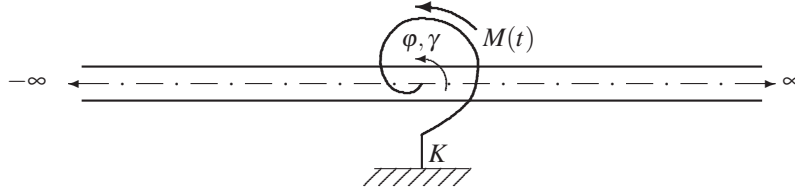


Figure 2 – Infinite beam supported by a single spring at  $x = 0$ .

dynamic stiffness derived for the Timoshenko and Euler-Bernoulli beam in Eqs. (22) and (48), respectively is shown in Fig. 3. As described above, the real part of the dynamic stiffness of the Timoshenko beam vanishes for excitation frequencies bigger than  $\tilde{\omega}_2$  with:

$$\tilde{\omega} = \sqrt{\frac{\kappa GA}{\rho I}} = 53607.8 \frac{1}{s}.$$

This is not the case for the Euler-Bernoulli beam. The real and imaginary part of the latter are identical. The rotational dynamic stiffnesses corresponding to the two different beam models agree reasonably only for small frequencies, approximately  $\omega < 10000 \frac{1}{s}$ . However, the stiffness curves differ strongly for large excitation frequencies. The linear asymptote of the imaginary part of the Timoshenko beam is also shown in Fig. 3. It can be seen, that Eq. (22) approaches the latter, whereas both the imaginary and real part of  $K_M$  corresponding to the Euler-Bernoulli model follow a square-root function of  $\omega$ .

In order to obtain a time-domain model, the low-frequency part of the rotational dynamic stiffness of the Timoshenko beam is approximated by the ratio of two polynomials (Eq. (31)) as described above. The agreement between the exact low-frequency vertical dynamic stiffness coefficient and rational approximations of degree  $M = 5$  and  $M = 9$  is shown in Fig. 4. Using the rational stiffness approximation, the rotation at the point of excitation of the coupled beam-spring system shown in Fig. 2 is described by the following system of first-order differential equations:

$$\tilde{\mathbf{A}}\mathbf{z}(t) + \mathbf{B}\dot{\mathbf{z}}(t) = \mathbf{r}(t), \quad (56)$$

with

$$\tilde{\mathbf{A}} = \text{tridiag} \begin{bmatrix} 1 & -1 & \dots & \mp 1 & * \\ K & -s_0^{(0)} & s_0^{(1)} & \dots & \pm s_0^{(M-1)} \\ * & 1 & -1 & \dots & \mp 1 \end{bmatrix}. \quad (57)$$

Here, the rotational spring stiffness  $K$  has been included at the position (1,1) of the matrix  $\tilde{\mathbf{A}}$ . The vector of unknowns  $\mathbf{z}$ , right-hand side vector  $\mathbf{r}$  and the matrix  $\mathbf{B}$  are identical to that given in Eqs. (39) and (40), respectively. Using Eq. (56), the rotation  $\varphi(x=0, t)$  due to a transient unit-impulse momentum,

$$i_0 = \int_0^h M(t) dt = 1.0 \text{ [Nm} \cdot \text{s]}, \quad (58)$$

acting within the time-intervall  $0 \leq t \leq h$  has been computed. The numerical results corresponding to different degrees of rational approximation are shown in Fig. 5. Although there is no analytical solution available, it can be seen, that the numerical solutions are approaching each other for increasing degree of approximation  $M$ .

According to the preceding section, Eq. (51), the coupled Euler-Bernoulli beam-spring system is described by the following fractional differential equation in the time-domain:

$$K \cdot \varphi(t) + 2\sqrt{2}EIC^{\frac{1}{4}} \left[ {}_{-\infty}D^{\frac{1}{2}}\varphi(t) \right] = M(t), \quad C = \frac{\rho A}{EI}. \quad (59)$$

Eq. (59) has also been solved numerically for a harmonic excitation,

$$M(t) = \hat{M} \cos \Omega t, \quad \hat{M} = 1.0 \cdot 10^6 \text{ Nm}, \quad \Omega = 20000 \frac{1}{s}, \quad (60)$$

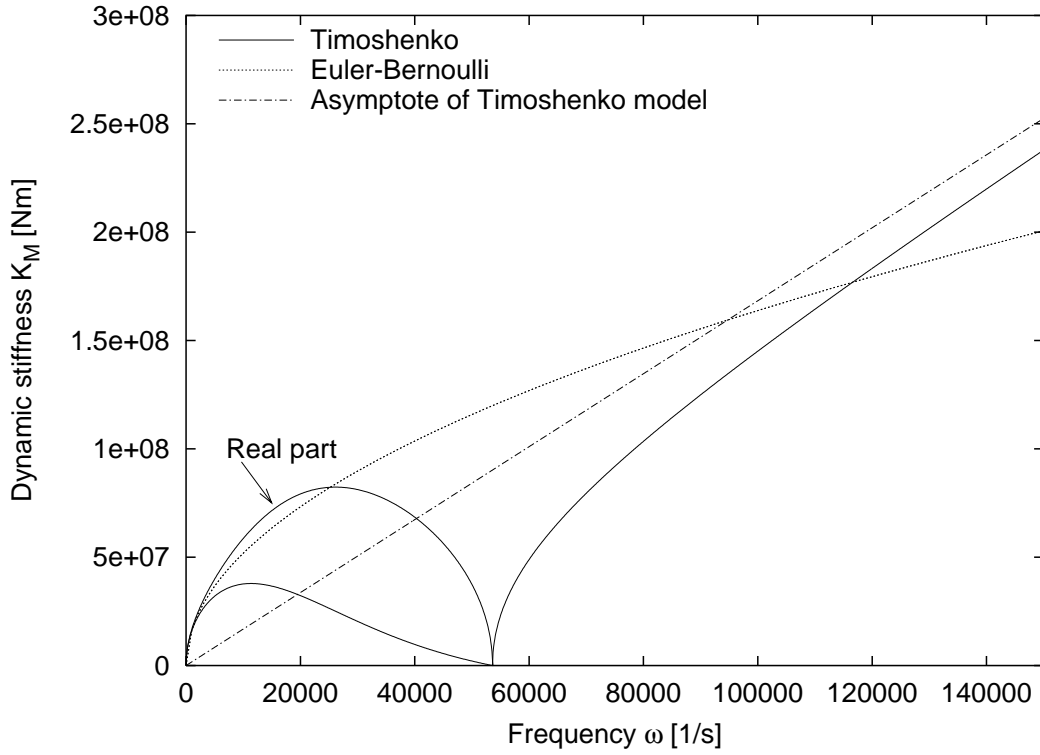


Figure 3 – Rotational dynamic stiffness for the Timoshenko and Euler-Bernoulli beam models

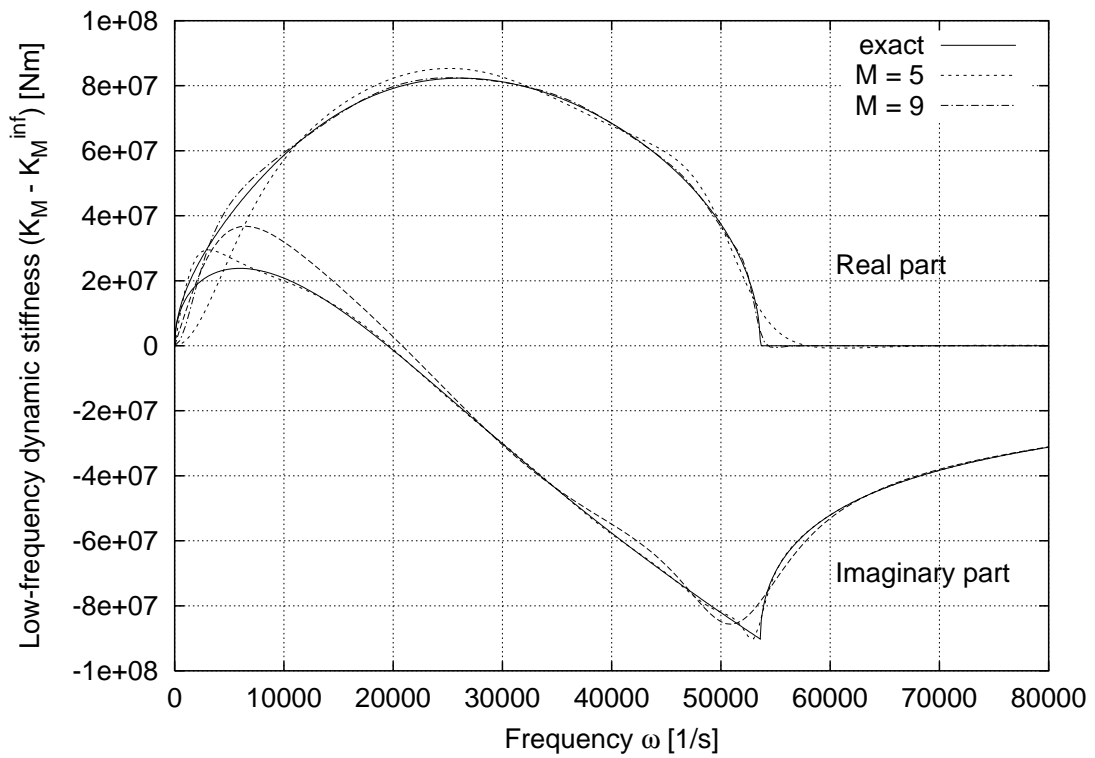


Figure 4 – Low-frequency part of the rotational dynamic stiffness of the Timoshenko beam

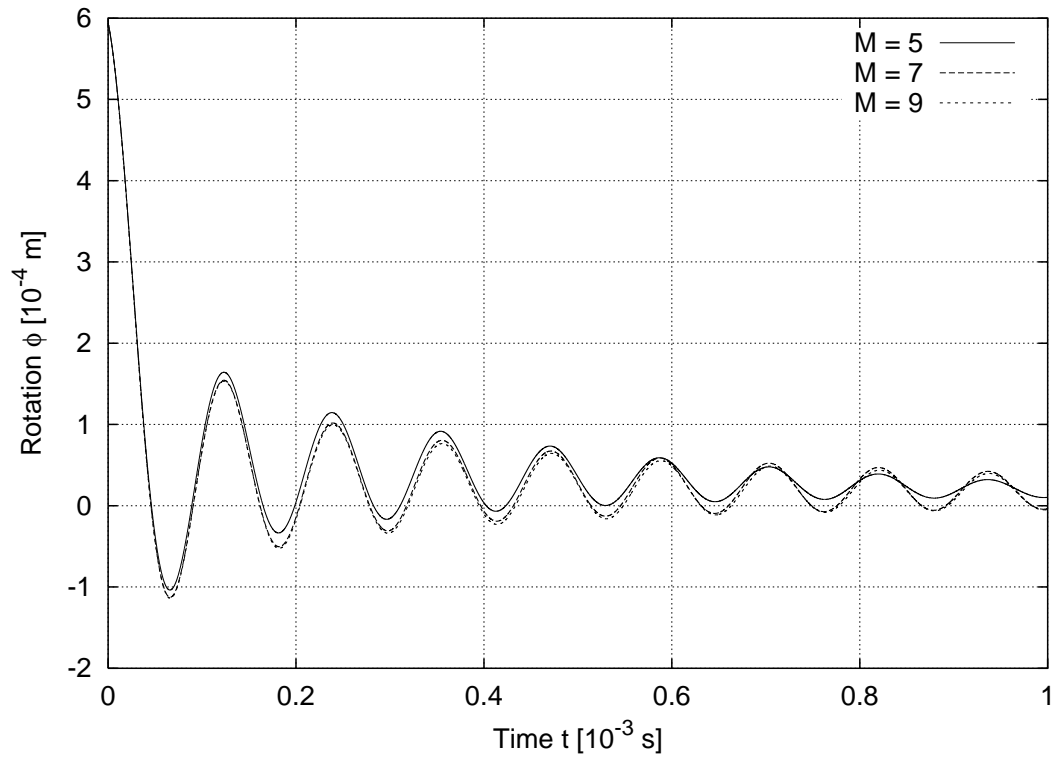


Figure 5 – Timoshenko beam supported by a single rotational spring  $K = 1.6 \cdot 10^7$  [Nm]. Rotation  $\varphi(x=0, t)$  due to unit-impulse load (58). Time step:  $h = 1.0 \cdot 10^{-7}$  s

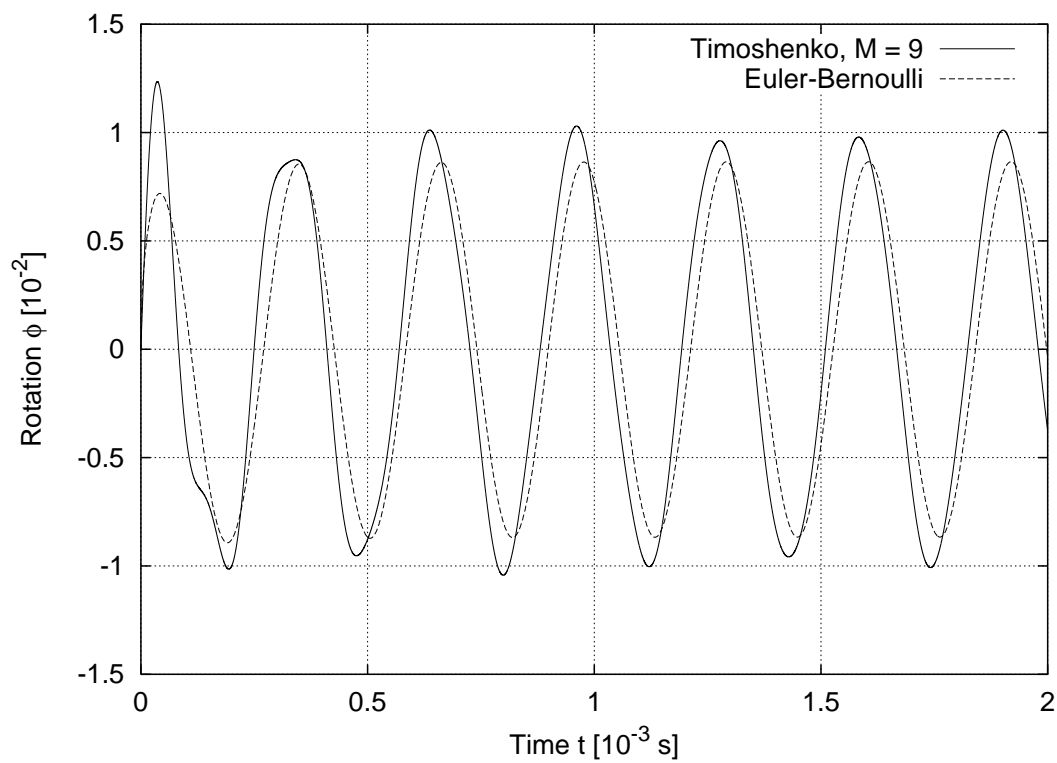


Figure 6 – Comparison of beam models in the time-domain. Rotation  $\varphi(x=0, t)$  due to harmonic excitation (60)

using a specific time-stepping scheme developed for fractional differential equations (Trinks, 2004; Ruge and Wagner, 1999). The resulting rotation  $\varphi(x = 0, t)$  at the point of excitation of the Euler-Bernoulli beam is compared to that of the Timoshenko beam in Fig. 6. It can be seen that the Euler-Bernoulli model leads to smaller rotations in this specific situation. Moreover, a phase shift is visible in Fig. 6. However, the numerically obtained displacement curves corresponding to the two different beam models are similar, despite the big differences with respect to the dynamic stiffness.

## CONCLUSIONS

Effects from shear deformations are well-known in structural statics. However, even if they are not significant from a mechanical point of view, they can improve the performance of the discretization scheme as is known from mixed methods in finite-element concepts in statics (Zienkiewicz and Taylor, 1994).

In structural dynamics of infinite domains the benefit from using Timoshenko's model is even greater: including the asymptotic behaviour in the formulation in the frequency-domain shows a linear dependency with respect to  $i\omega$  and thus corresponds to a first-order time-derivative. Consequently, the solution in the time-domain can be done by classical time-solvers with local properties. Contrary to shear models, Euler-Bernoulli's theory generates rational powers of  $i\omega$  in the frequency-domain and therefore fractional derivatives in the time-domain which ask for non-local time-solvers.

## REFERENCES

- Antes H., Schanz M., Alvermann S., 2004, "Dynamic analysis of plane frames by integral equations for bars and Timoshenko beams", *Journal of Sound and Vibration*, Vol.276, pp. 807-836
- Beskos D.E., 1987, "Boundary element methods in dynamic analysis", *Applied Mechanics Reviews (ASME)*, Vol.40, pp. 1-23.
- Beskos D.E., 1997, "Boundary element methods in dynamic analysis: Part II (1986-1996)", *Applied Mechanics Reviews (ASME)*, Vol.50, pp. 149-197.
- Bettess P., 1992, "Infinite Elements", *Penshaw Press: Sunderland*.
- Cowper, G.R., 1966, "The shear coefficient in Timoshenko's beam theory", *ASME Journal of Applied Mechanics*, Vol.33, pp. 335-340.
- Fung, Y.C., 1986, "Foundations of Solid Mechanics", *Prentice-Hall, Englewood Cliffs*, pp. 322-325.
- Givoli D., 1999, "Exact representations on artificial interfaces and applications in mechanics", *Applied Mechanics Reviews (ASME)*, Vol.52(11), pp. 333-349.
- Harari I., 2006, "A survey of finite element methods for time-harmonic acoustics", *Computer Methods in Applied Mechanics and Engineering*, Vol.195, pp. 1594-1607.
- Hörmander L., 1963, "Linear Partial Differential Operators", *Springer, Berlin*.
- Kausel E., 1988, "Local transmitting boundaries", *Journal of Engineering Mechanics (ASCE)*, Vol.114, pp. 1011-1027.
- Mindlin, R.D., Deresiewicz, H., 1953, "Timoshenko's shear coefficient for flexural vibrations of beams", Report No. 10, ONR Project NR064-388, Department of Civil Engineering, Columbia University, New York.
- Podlubny I., 1999, "Fractional differential equations", Volume 198 in *Mathematics in Science and Engineering*, Academic Press.
- Ruge P., Wagner N., 1999, "Time-domain solutions for vibration systems with fading memory", *European Conference on Computational Mechanics*, Munich, Germany, pp.367-374, published on CD-ROM.
- Ruge P., Trinks C., Witte S., 2001, "Time-domain analysis of unbounded media using mixed-variable formulations", *Earthquake Engineering and Structural Dynamics*, Vol.30, pp. 899-925.
- Ruge P., Trinks C., 2003, "Dynamics of infinite beams described by fractional time derivatives", *ASME 19th International Biennial Conference on Mechanical Vibration and Noise*, Chicago, Illinois, published on CD-ROM.
- Ruge P., Trinks C., 2004, "Consistent modelling of infinite beams by fractional dynamics", *Nonlinear Dynamics*, Vol.38, pp. 267-284
- Ruge P., Birk C.; probably 2007, "Radiation damping in infinite beams", submitted to *Journal of Sound and Vibration*.
- Song C., Wolf J.P., 1997, "The scaled boundary finite-element method - alias consistent infinitesimal finite-element cell method - for elastodynamics", *Computer Methods in Applied Mechanics and Engineering*, Vol.147, pp. 329-355.
- Trinks C., 2004, "Consistent absorbing boundaries for time-domain interaction analyses using the fractional calculus", PhD Thesis, Technische Universität Dresden, Fakultät Bauingenieurwesen.
- Wolf J.P., 1986, "A Comparison of Time-Domain Transmitting Boundaries", *Earthquake Engineering and Structural Dynamics*, Vol.14, pp. 655-673.
- Wolf J.P., 2003, "The Scaled Boundary Finite Element Method", *Wiley: Chichester*.
- Zienkiewicz O.C., Taylor R.L., 1994, "The finite element method", Vol. 1, 4th ed., *McGraw Hill*.

## RESPONSIBILITY NOTICE

The author(s) is (are) the only responsible for the printed material included in this paper.